View metadata, citation and similar papers at core.ac.uk

brought to you by CORE

provided by NASA Technical Reports Server

"Made available under NASA sponsorship
In the interest of early and wide dissemination of Earth Resources Survey
Program information and without liability
for any use made thereof."

E 7.3 10.447
CR-131242

MAPPING ARCTIC SEA ICE FROM THE EARTH RESOURCES TECHNOLOGY SATELLITE

by

James C. Barnes and Clinton J. Bowley

ENVIRONMENTAL RESEARCH & TECHNOLOGY, INC.
529 Marrett Road, Lexington, Massachusetts 02173

(E73-10447) MAPPING ARCTIC SEA ICE FROM THE EARTH RESOURCES TECHNOLOGY SATELLITE (Environmental Research and Technology, Inc.) 19 p HC $3.00 CSCL 08L

N73-20407

Unclas
G3/13 00447

The research described in this paper was supported by the National Aeronautics and Space Administration under Contract No. NAS 5-21802. The NASA Scientific Monitor for the contract is Mr. James R. Greaves, of Goddard Space Flight Center.

Details of illustrations in this document may be better studied on microfiche

Original photography may be purchased from:
EROS Data Center
10th and Dakota Avenue
Sioux Falls, SD 57198

ABSTRACT

This paper surveys the use of the high-resolution, multispectral data from ERTS-1 (Earth Resources Technology Satellite) for mapping Arctic sea ice. Methods for detecting ice and for distinguishing between ice and cloud are discussed, and examples of ERTS data showing ice distributions in northern Hudson Bay, M'Clure Strait, the eastern Beaufort Sea, and the Greenland Sea are presented. The results of the initial analysis of ERTS data indicate that the locations of ice edges and ice concentrations can be accurately mapped, and that considerable information on ice type can be derived through use of the various spectral bands. Ice features as small as 80 to 100 m width can be mapped.

1. INTRODUCTION

Sea ice could be detected in pictures of the earth taken by the earliest TIROS meteorological satellites more than a decade ago. By the mid 1960s, information obtained from satellites was being incorporated into ice charts and was even being used to route an occasional ship through the ice. In fact, in 1966, Fletcher stated that the "observational barrier" in the Arctic was crumbling primarily under the impact of satellite observation systems. Now, for the first time, ERTS-1 (Earth Resources Technology Satellite) is providing multispectral data at a resolution that has previously not been available. This paper describes the results of the initial evaluation of these data for detecting and mapping sea ice. The techniques being developed in studies such as this will lead eventually to the use of operational satellite systems to collect ice data on a far more complete and economical basis than has heretofore been possible.

Although studies such as those reported by McClain and Baliles (1971) and Barnes, Chang and Willand (1972) have demonstrated that useful sea ice information can be acquired from existing meteorological satellite systems, nevertheless, serious limitations in the use of these data do exist. In particular, the spatial resolutions of the sensors are adequate only for detecting gross ice boundaries and do not permit the mapping of small-scale features such as leads and polynyas, which may be especially critical for heat-balance considerations. Furthermore, intermediate ice concentrations cannot be mapped with the reliability desired by scientific and operational personnel, and icebergs, except for the largest Antarctic tabular bergs, cannot be detected.

ERTS-1 was placed into a near-polar, sun-synchronous orbit at a height of 900 km on 23 July 1972. Except for a brief period in early August, the MSS (Multi-Spectral Scanner) sensor system has operated continuously, returning approximately 188 data scenes each day, 44 of which are over the United States. The MSS views a swath 180 km wide, with coverage of the exact same area occurring every 18 days. Because of orbital overlap at the higher latitudes, however, coverage of Arctic areas can occur as often as three or four consecutive days during each 18-day cycle. The initial studies of the data have indicated that features greater than about 70 m in width can be identified and can be mapped accurately to a scale of at least 1:250,000. The MSS senses in four spectral bands: MSS-4 (0.5 to 0.6 μm), MSS-5 (0.6 to 0.7 μm), MSS-6 (0.7 to 0.8 μm), and MSS-7 (0.8 to 1.1 μm).

2. SEA ICE DETECTION

Analysis of ERTS-1 data from the Arctic during the period between late July and late October 1972 indicates that sea ice can be identified in all of the MSS spectral bands because of its high reflectance. It has been found, however, that the photographic processing of prints from the original 70 mm negatives can be important for ice detection, since exposures selected to retain detail in bright, snow-covered land areas may result in the loss of significant ice features. Although ice and clouds may have similar reflectances, ice can be distinguished through the following interpretive keys:

- The brightness of ice fields and large ice floes is often more uniform than that of clouds. Furthermore, ice floes and features such as leads and fractures within an ice field can at times be detected through thin cirriform cloud cover.
- Cloud shadows can often be detected on the underlying ice surface.
- Edges of most ice features, particularly ice floes, are more distinct than edges of clouds.
- Ice cover fits coastlines and islands, permitting land features to be recognized.
- The spatial frequencies of ice features are not characteristic of cloud patterns. These features include ice floes surrounded by broken ice, narrow ice bands, and spiral patterns induced by ocean currents.

- When repetitive coverage is available, some ice features remain stable over the 24-hour interval between observations. Even at the longer periods between ERTS cycles, some large floes can still be identified.

3. MAPPING OF ICE FEATURES

Ice features have been mapped for several Arctic areas including the eastern Beaufort Sea, parts of the Canadian Archipelago, and the Greenland Sea. The ice edges and ice concentration boundaries have been mapped. Tentative identification of ice types and types of ice surface features has been made, based on variations in reflectance and the shapes and sizes of the patterns. Differences in reflectance between the shorter wavelength bands (MSS-4 and MSS-5) and the near-IR band (MSS-7) have been found very useful for differentiating ice types. When available, aerial-survey ice charts have been used as correlative data. Examples of the application of ERTS data to ice mapping are presented in the following sections.

Northern Hudson Bay

The MSS-5 imagery covering a part of northern Hudson Bay on 27 July is shown in Figure 1. A well-defined, irregular ice edge is evident extending southwestward from Coats Island, with several bights and tongues apparently caused by a westerly surface wind flow. The ice along the immediate ice edge appears to consist mostly of brash or rotten ice, whereas the ice east of the edge consists of varying concentrations of vast, big, or medium category ice floes. An ice belt is visible off the south coast of Southampton Island, and fast ice together with some vast ice floes are located along and just off the north coast of Coats Island. (NOTE: Ice

floes are defined in the WMO Sea Ice Nomenclature (WMO Pub. No. 259, TP. 145) as follows: Giant Floe - over 10 km (6.3 n.mi.) across; Vast Floe - 2 to 10 km across; Big Floe - 500 to 2000 m across; Medium Floe - 100 to 500 m across; Small Floe - 20 to 100 m across).

The ice features mapped from the ERTS data are in good agreement with the conditions reported in ice charts (supplied by the Canadian Ice Forecasting Central) for the last week in July. These charts indicate a sharp, irregular (bights) ice edge extending southwest of Coats Island with ice-free water to the west, and an ice belt south of Southampton Island composed of 3/10's of first year ice of which 1/10 is medium or larger size floes. The area northwest of Coats Island in Fisher Strait is shown to be comprised of 5/10's of first year ice of which 2/10's is medium or larger size floes.

M'Clure Strait

Images from the near-IR spectral band (MSS-7) for two ERTS passes crossing the M'Clure Strait area, including parts of Prince Patrick, Eglinton, and Melville Islands to the north and Banks Island to the south, are shown in Figures 2 and 3. These data indicate that significant changes in the ice conditions in M'Clure Strait have occurred during the five-week interval between the time of the first pass, 29 July, and the second, 4 September. On the earlier date, fast ice exists along the northern and northwest coasts of Banks Island. Shore leads are observed, however, particularly near the mouths of the rivers that empty into M'Clure Strait along the northern coast of the island. Much of M'Clure Strait is covered by fast ice, although at the western end of the strait numerous fractures and leads can be detected. The structure of the ice breakup process seems to be evident in this imagery; fractures extending through the ice between

Eglinton Island and Banks Island open into leads farther west and eventually into larger open water areas.

A considerable amount of detail on the ice surface is also evident in Figure 2. Particularly noticeable are the dark areas in Crozier Channel and Kellett Strait along the coasts of Prince Patrick and Melville Islands. These areas do not appear as dark in the MSS-4 spectral band (not shown). Because of the differences in reflectance in the MSS-4 and MSS-7 images, these areas are believed to be areas where the ice surface has been blown free of snow cover and is now covered by melt water. As pointed out by McClain (1972), even a thin film of water on the ice can cause a sharp drop in reflectance in the near-IR portion of the spectrum, whereas in the visible the reflectance does not change significantly. Daytime temperatures during this period at Mould Bay, located on Prince Patrick Island, are reported to be well above freezing. Several smaller, very dark spots can also be detected in the ice in M'Clure Strait; these spots are dark in the MSS-4 imagery as well, so are deduced to be areas that contain open water rather than melt water on the ice.

The bright features and linear patterns that interlace the ice surface, even in the dark areas discussed above, may be associated with ridging and hummocking of the ice. On this date the islands are essentially snow-free, and some cloudiness covers the eastern part of M'Clure Strait and Melville Island. The clouds can easily be distinguished because of their shadows.

Five weeks later (Figure 3), the entire ice sheet in M'Clure Strait has broken up. No fast ice is evident, except along Prince Patrick Island and in Crozier Channel and Kellett Strait. Open water exists along the coast of Banks Island, and breaks in the ice can be seen throughout M'Clure Strait. The ice concentration appears to be close (6 to less than 7 oktas)

or very close pack ice (7 to less than 8 oktas), consisting of ice floes surrounded by brash ice. The individual floes are distinctly brighter than the surrounding brash ice in the MSS-7 data. Considerable cloudiness covers the northern part of the area, and cloud shadows can be seen on the ice in M'Clure Strait, even though the clouds themselves are nearly transparent. By this date, a part of Banks Island and the higher terrain of Melville Island have again become snow covered.

Eastern Beaufort Sea

Sea ice concentrations in the eastern Beaufort Sea in the area from 72° to 75°N and 132° to 138°W were mapped from ERTS data on two dates during August. An enlargement of a part of the MSS-7 scene covering the area near 74°N, 130°W on 2 August is shown in Figure 4; an enlargement of the MSS-7 scene covering nearly the same area on 22 August is shown in Figure 5. Each of these enlargements covers an area about 100 km across.

In the 2 August data, a total of 13 very large "giant floes" (up to 50 km across) can be identified within the area mapped. These floes are surrounded by ice concentrations consisting primarily of open pack (3 to less than 6 oktas) and close pack (6 to less than 7 oktas), with many various sized smaller floes. Twenty days later, the same 13 giant floes can be identified because of their shapes and surface features. Three of these floes can be seen in Figures 4 and 5. Significant deterioration has occurred in only two of the 13 floes; in these two floes, large areas (about 1/4 of the original floe size) have apparently broken off their southern edges and broken into smaller floes. In the 20-day period, however, the overall ice concentrations appear to have increased somewhat and now consist mostly of close pack and very close pack (7 to 8 oktas). This apparent increase in ice concentration is probably the result of the overall breakup of the

numerous smaller "giant floes" (10 to 20 km across), which are greatly reduced in number in the 22 August data. Measurements of the motion of the 13 floes over the 20-day period indicated a mean direction of motion toward the southwest, with a clockwise shift in the direction of motion from north to south; in addition to moving in a more westerly direction, the southernmost flows also moved more slowly. The measured speeds range from 2.8 to 4.3 km per day.

In the MSS-7 data shown in Figures 4 and 5, numerous surface features can be detected in the larger ice floes. As in M'Clure Strait, the dark features are believed to be associated with fractures and areas containing puddles and thaw holes, whereas the brighter features are ridges and hummocks. A comparison of the surface features of the individual floes indicates that noticeable changes do occur over the 20-day period. In particular, although the larger dark features can be readily identified on both dates, many of the smaller dark spots observed in 2 August are not visible on 22 August. This might indicate that the smaller spots are puddles that have refrozen during the intervening period. However, temperature records for the stations nearest this area show that freezing did not begin until late August or early September. It does not seem possible, therefore, that the puddles could have refrozen. A tentative suggestion offered by W. E. Markham, of the Canadian Ice Forecasting Central, is that the puddles may have drained through cracks and small holes too small to be detected at the ERTS resolution. It is possible, however, that some other action is also taking place.

Greenland Sea (Along East Coast of Greenland)

ERTS imagery of the eastern coastal area of Greenland on several dates during September and early October display wide variations in ice types

and concentrations, including compacted belts and eddies that apparently result from the combined effects of current flow and surface wind. An example is given in Figure 6 (a and b), where the MSS-4 and MSS-7 images (slightly enlarged) covering the area near 77°N on 25 September are shown. In these scenes, the coast of Germania Land and the northern end of Store Koldeway are at the left. A shore lead of about 2 km width exists along the coast, and open water exists south of Germania Land into Dove Bugt. An open water area also exists southeast of a giant ice floe (about 25 km across) located near the top of the respective images. This clearing out of the ice is presumed to be primarily the result of a wind flow from the northwest.

A comparison between Figures 6a and 6b reveals distinct differences in the sea ice characteristics in the two spectral bands. The ice in the eastern part of this scene appears much brighter in the MSS-4 band than in the MSS-7. Closer to the coast, the area of very close and consolidated pack ice has a nearly uniform reflectance in the MSS-4 band, whereas in the MSS-7 band the individual ice floes are distinctly brighter than the surrounding ice. This is particularly evident in the ice adjacent to the shore lead, which appears fairly bright in the MSS-4 band, but is nearly black in the MSS-7 band. Similarly, in the large ice floe near the top of the scene and in several of the smaller floes near the bottom, dark spots in the MSS-7 band are either much lighter or cannot be detected at all in the MSS-4 band.

As discussed earlier in the paper, differences in reflectance in the two spectral bands are believed to be due to the existence of melt water on the ice and, thus, open water can be distinguished from puddled areas. The imagery shown in Figure 6 also indicates that certain ice-covered areas have a significantly lower reflectance in the MSS-7 band. These areas are

presumably areas of brash or rotten ice, where a greater amount of water exists on and around the ice elements. Thus, whereas the total extent of the ice can be mapped better from the visible data, the combined use of the visible and near-IR data can distinguish certain ice types.

4. CONCLUSIONS

The results of the initial analysis of data from ERTS-1 indicate that sea ice is detectable in all of the ERTS MSS spectral bands and can be distinguished from clouds through a number of interpretive keys. The photographic processing of prints from the original 70 mm negatives can be important for ice detection, however, since exposures selected to retain detail in land areas may result in the loss of significant ice features. Overall, the MSS-4 (0.5 to 0.6 μm) and MSS-5 (0.6 to 0.7 μm) bands appear to be better for mapping the ice edge, whereas the MSS-7 (0.8 to 1.1 μm) band provides greater detail in the ice features. Moreover, the multispectral analysis of the ERTS visible and near-IR bands provides much information on ice type and ice surface features that cannot be derived from a single band.

The locations of ice edges and the ice concentrations mapped from ERTS data are in good agreement with the rather limited amount of correlative data available to date. The ice types that can be tentatively identified in ERTS data include fast ice, pack ice of various concentrations, ice floes ranging from the "giant flow" down to the larger sized "small floe", brash ice, rotten ice, leads, fractures, puddled areas, areas of thaw holes, and flooded ice. Although larger icebergs can be seen, it is difficult to distinguish them from ice floes; however, icebergs embedded in areas of

fast ice can, at times, be detected because of their shadows on the surrounding ice. Ice floes and fractures as small as 80 to 100 m in width have been mapped. Moreover, when repetitive cloud-free ERTS coverage is available, ice elements can be identified over 24-hour periods, enabling their movements to be measured; some large flows have been recognized over intervals of as long as 20 days, enabling mean ice movements over long periods to be determined.

5. REFERENCES

Barnes, J. C., D. T. Chang, and J. H. Willand, 1972: "Image Enhancement Techniques for Improving Sea Ice Depiction in Satellite Infrared Data," Journal of Geophyisical Research; Oceans and Atmospheres Edition, 77(3), pp. 453-462.

Fletcher, J. O., 1966: "Forward," Proc. of Symposium on the Arctic Heat Budget and Atmospheric Circulation, Memorandum RM-5233-NSF, The RAND Corporation.

McClain, E. P., 1972: "Detection of Ice Conditions in the Queen Elizabeth Islands," Proc. of Symposium on Earth Resources Technology Satellite-1, September 29, 1972, National Aeronautics and Space Administration.

McClain, E. P., and M. D. Baliles, 1971: "Sea Ice Surveillance from Earth Satellites," Mariners Weather Log, 15(1), pp. 1-4.

FIGURE CAPTIONS --

Figure 1 ERTS-1 MSS-5 imagery of northern Hudson Bay, 27 July 1972. Southampton Island (A), Coats Island (B).

Figure 2 ERTS-1 MSS-7 imagery of M'Clure Strait, 29 July 1972. Prince Patrick Island (A), Eglinton Island (B), Melville Island (C), Banks Island (D).

Figure 3 ERTS-1 MSS-7 imagery of M'Clure Strait, 4 September 1972. Note changes in ice conditions as compared to Figure 2, 5 weeks earlier.

Figure 4 Enlargement of ERTS-1 MSS-7 image of eastern Beaufort Sea, near 74°N, 130°W, 2 August 1972. Three ice floes that can also be identified in an ERTS image 20 days later are indicated. Floe A is about 50 km in width; some cloud shadows can be detected on floe C.

Figure 5 Enlargement of ERTS-1 MSS-7 image covering approximatly the same area as shown in Figure 4, 22 August 1972. Floes A, B and C and some other smaller floes can also be identified in Figure 4.

Figure 6a Enlargement of ERTS-1 MSS-4 image (visible spectral band) of East Coast of Greenland, near 77°N, 25 September 1972, Germania Land (A), Store Koldeway (B), and Dove Bugt (C).

Figure 6b Enlargement of ERTS-1 MSS-7 image (near IR spectral band) of same scene as in Figure 6a. Note the differences in reflectance of ice features as compared to the visible data.

ERTS Image Identifier Numbers —

Figure 1 1004-16322-5, 1004-16324-5

Figure 2 1006-20060-7, 1006-20062-7

Figure 3 1043-20120-7, 1043-20122-7

Figure 4 1010-20293-7

Figure 5 1030-20410-7, 1030-20412-7

Figure 6a 1064-13354-4

Figure 6b 1064-13354-7

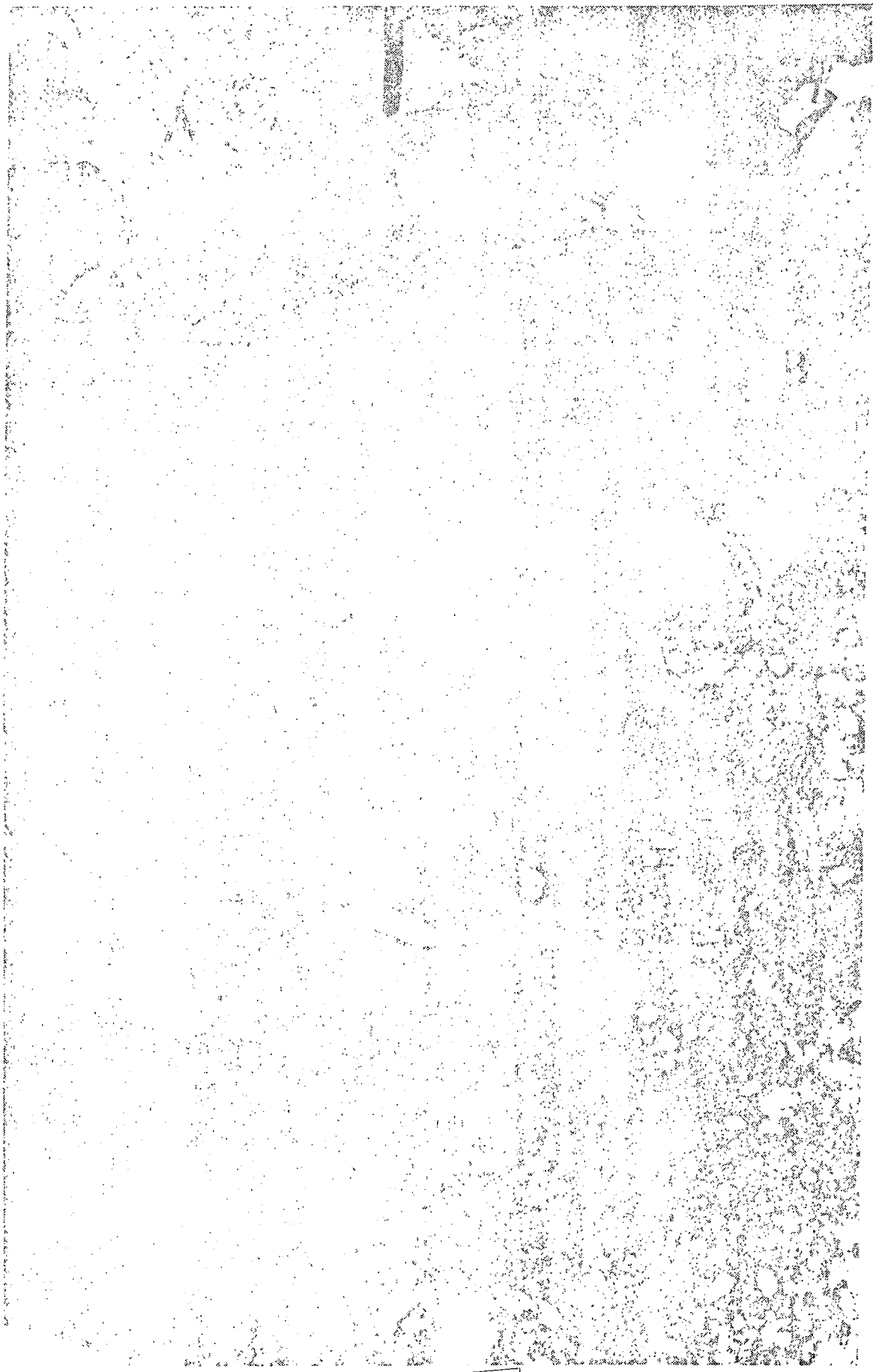

Reproduced from
best available copy.

Reproduced from
best available copy.

Reproduced from
best available copy.

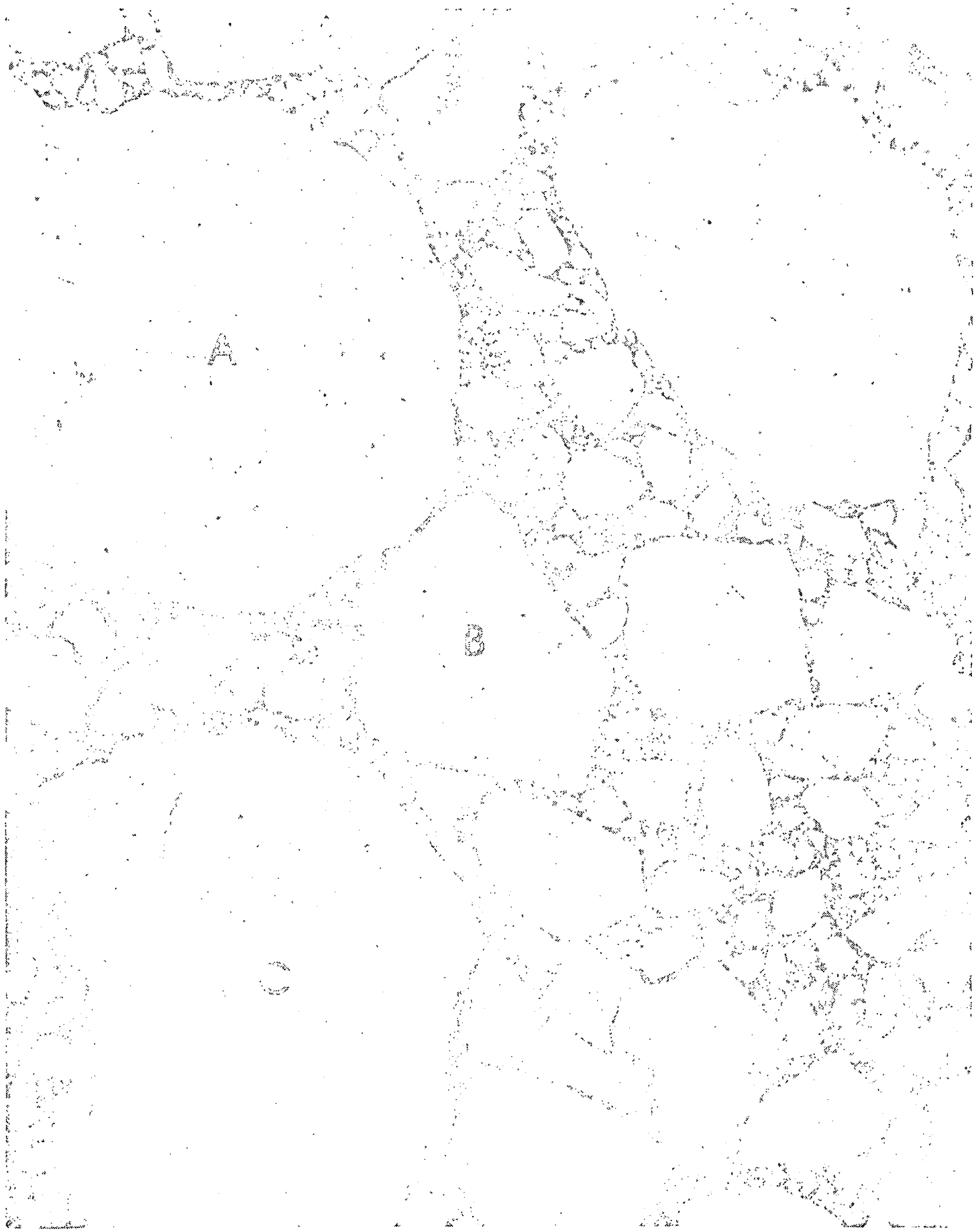

Reproduced from best available copy.

Reproduced from
best available copy.

6b

6a

Reproduced from
best available copy.